JOURNAL OF MATERIALS SCIENCE **37** (2002) 3747–3758

Microstructure and properties of alumina-SiC nanocomposites prepared from ultrafine powders

D. SCITI
CNR-IRTEC, Via Granarolo 64, I–48018, Faenza

J. VICENS
LERMAT-ISMRA, 6 Bd. Maréchal Juin, F-14050, Caen

A. BELLOSI
CNR-IRTEC, Via Granarolo 64, I–48018, Faenza
E-mail: bellosi@irtec1.irtec.bo.cnr.it

Alumina-Silicon Carbide nanocomposites were produced and studied under different aspects: characteristics of the starting materials, processing, microstructure and mechanical properties. The raw materials were two kinds of fine SiC powders (30 and 45 nm) and two Al_2O_3 powders (60 and 140 nm). Different compositions (amounts of SiC in the range 0.5–5 vol%) were performed and the characteristics of the resulting materials compared. The oxygen enrichment in SiC nanopowder due to specific powder treatments was controlled, in order to optimize powder processing routes. Densification tests of Al_2O_3-SiC powder mixtures were performed both by pressureless sintering and hot pressing route. The addition of SiC reduced the densification rate and favoured a refinement of the matrix. Improvement of mechanical properties over monolithic alumina was obtained in composites with the 45 nm SiC. The study pointed out that the critical factor for the success of these materials is the choice of the raw SiC powders in terms of grain size and state of agglomeration. The addition of this ultrafine SiC strongly affected the microstructural evolution, even at low volumetric fractions. The results do not substantiate any remarkable effect by dispersoids in the tested nanosize range.

1. Introduction

The class of materials known as nanocomposites has been extensively studied over the past ten years [1–20], mainly due to the great mechanical performance obtained by Niihara and his co-workers [1–4]. In particular the most impressive results concern the composite Al_2O_3 with addition of 5 vol% SiC that exhibited an improvement of 300% for strength and of 50% for toughness over monolithic alumina [1]. The SiC powder used in that study has a mean particle size in the range 200–300 nm. Many researchers tried to reproduce these materials and studied the numerous factors that influence the final properties. Recently, Sterniztke has reviewed and compared all the studies in literature [5].

Conventional processing routes concerning powder treatment and densification are not always efficient for nanophase materials. Small differences in the processing procedure can have a pronounced effect on the microstructure and properties [6–8]. In order to benefit by the potentialities deriving from the introduction of ultrafine particles in an alumina matrix, the principal aim to achieve is a homogeneous dispersion of the second phase. Mean grain size and distribution of the SiC particles are critical factors as they affect the location of the particulate in the matrix [9–11]. It was reported [9] that SiC particles <150 nm, detached from advancing grain boundaries, are dispersed within the matrix grains, while larger SiC particles are found mainly in intergranular positions. Finally, the amount of oxygen on SiC particle surface induced during powder treatment must be carefully controlled as it results in liquid phases during sintering and glassy intergranular phases in the dense materials.

Although the results of Niihara have not been reproduced by other researchers, various studies on Al_2O_3/SiC nanocomposites have shown a significant increase in strength over monolithic alumina, generally accompanied by a modest increase in toughness [9–13]. Although intragranular fracture and increased wear resistance are a plain indicator of grain boundary reinforcement, the actual strengthening and toughening mechanisms remain unclear [5]. In this respect, different hypotheses have been indicated: refinement of the matrix due to grain boundary pinning by the SiC particles, change in the processing flaw type (from Al_2O_3 typical void-like flaws to crack-like flaws), creation of dislocation networks, crack healing after annealing. Several models dealing with these phenomena have been developed; according to Niihara [1–3] strength improvement is mainly due to the refinement of the matrix in the nanocomposite with respect to

monolithic alumina. It is more difficult to identify the toughening mechanisms in these materials, as the observed improvements are small or even absent. Toughening can be achieved through *R*-curve effects, crack deflection at the SiC particles, grain boundary strengthening caused by thermal expansion mismatch between SiC and Al_2O_3 and/or internal stresses. However all these mechanisms highly depend on processing procedures and microstructural details [5].

According to a completely different approach, several scientists stand up for no synergistic effect by nanosized particulate [12, 21, 22]. The improvement in mechanical properties may either be related to residual microstresses stored in the material after sintering or even be affected by extrinsic factors related to the sample preparation or testing procedure, rather than being an inherent material property.

In this study Al_2O_3-based nanocomposites were produced from different kinds of powders. The starting aluminas were commercial powders with different mean particle size, i.e., 140 and 60 nm. The ultrafine SiC powders had 30 and 45 nm of mean particle size, which means that the nanophase particles were four/five times finer than those generally used in most of the studies found in literature [1, 6–8]. The fraction of SiC particles was varied between 0.5 and 5 vol%. The modification of oxygen content in the finest SiC powder was analyzed after specific powder treatments in order to avoid additional oxidation during the preparation of the Al_2O_3-SiC powder mixtures. The microstructure and properties of these nanocomposites were studied and discussed.

2. Experimental

The starting materials were: two commercial α-Al_2O_3 powders: Ceralox HPA 0.5 (labelled *coarse*) and Baikalox CR30 (labelled *fine*), and two types of nanosized β-SiC powders labelled SiC1 (produced by ENEA, Italy) and SiC2 (produced by CEA-Saclay, Vitry Sour Seine, France) obtained via a laser route. The main characteristics of the powders are reported in Table I.

Chemical analyses and TEM analyses were performed on SiC powders to determine the amount of oxygen and the silica layer thickness. In order to evaluate the surface reactivity of the nanoparticles during processing steps, the raw SiC powders were treated in aqueous environment (at R.T.) at pH = 6, for 12 h, following a processing method generally employed in other studies to homogenize the Al_2O_3-SiC powder mixtures [23]. In addition, a powder sample of raw SiC2 was heat treated in graphite furnace under Ar at 1300°C 12 h. After each treatment, the variation of the surface silica was evaluated through chemical analysis, as reported in Table I. TEM and HRTEM analyses were also performed on SiC2 powder.

Different amounts of silicon carbide were added to the alumina powder, i.e., 0.5, 2.0, 5.0 vol%. Monolithic alumina was also produced for comparison. The compositions are summarized in Table II. On the basis of the results presented in the next section, water-based solvents were considered unsuitable to homogenize the powder mixtures of Al_2O_3 and SiC. Therefore, the mixtures were prepared through separate dispersions of the starting powders in ethyl alcohol by ultrasonic pulses associated with magnetic stirring. The batches were then mixed and further homogenized by ultrasonic pulses. Drying was performed in a rotary evaporator under an inert gas stream and then the powders were passed through a plastic sieve (150 μm). Hot pressing was performed under vacuum (10^{-1} Pa) at temperatures in the range 1670–1700°C, for 10–20 minutes of soaking time and with an applied pressure of 30 MPa (Table II).

For pressureless sintering tests, the mixture were further treated in hexane with 2 wt% of a phosphate ester (Enphos PS21A) + 2 wt% trioleine in order to achieve a suitable green density. Green pellets were prepared by die pressing at 100 MPa and cold isostatic pressing at 380 MPa, and then sintering was carried out in graphite furnace under Ar or N_2 at various temperatures (1600–1800°C) with 1–4 h of holding time.

TABLE I Characteristics of the starting powders (s. s. a. = specific surface area, m.g.s. = mean grain size, S = surface silica layer thickness)

	s. s. a. (m^2/g)	m. g. s. (μm)	Density (g/cm^3)	Purity (%)	Chemical composition
Al_2O_3 coarse	11	140	3.95	99	p.p.m. Na:26 Si:24 Fe:9 Ca:10 Mg:8
Al_2O_3 fine	27	60	3.89	99.9998	
SiC1 as received	42	45	3.21	[a]O:3.4 SiO_2:6.4 wt% S ~ 0.7 nm	[a]wt% Si:67.6, C:29.0, O:3.4
SiC1 after 12 h at 1300°C under Ar	"	"	–	[a]O:3.7 SiO_2:6.8 wt% S ~ 0.7 nm	–
SiC2 as received	63	30	3.2	[a]O:3.94 SiO_2:7.4 wt% S ~ 0.5 nm	[b]At% Si:48.3, C:48.4, O:3.3
SiC2 after 12 h at 1300°C under Ar	"	"	–	[a]O:4.74 SiO_2:8.9 wt% S ~ 0.6 nm	[b]At% Si:50.31, C:43.65, O:5.99
SiC2 after 12 h in water at pH = 6	"	"	–	[a]O:6.18 SiO_2:11.6 wt% S ~ 0.75 nm	[b]At% Si:49.9, C:46.7, O:3.4

[a]From chemical analysis.
[b]From TEM + EDS analyses (mean values of 10 measurements).

TABLE II Compositions, raw powders, hot pressing parameters ($P = 30$ MPa) used to produce dense composites. Density of the hot pressed samples and mean grain size of the matrix alumina

Sample	Composition	Materials		H. P. cycle (°C/min)	Density		Matrix m.g.s. (μm)
		Al_2O_3	SiC		(g/cm^3)	(%)	
A5*	$Al_2O_3 + 5$ vol% SiC	Coarse	SiC1	1700/15	3.86	99	0.34
A*	Al_2O_3	Coarse	–	1450/25	3.94	100	1.2
A5	$Al_2O_3 + 5$ vol% SiC	Fine	SiC2	1700/20	3.87	99	0.3–0.4
A2	$Al_2O_3 + 2$ vol% SiC	Fine	SiC2	1670/10	3.84	99	0.4–0.5
A0.5	$Al_2O_3 + 0.5$ vol% SiC	Fine	SiC2	1650/10	3.88	100	~0.6
A	Al_2O_3	Fine	–	1450/25	3.89	100	~0.9

Al_2O_3 coarse: Ceralox HPA0.5; fine: Baikalox CR30.

The density of the sintered materials was measured through the Archimede method in distilled water. The crystalline phases were determined by X-ray diffraction. The samples were cut and polished to 1 micron for SEM observation. Thermal etching was carried out in a graphite furnace at 1350°C in atmosphere of Argon in order to delineate the grain boundaries. SEM-EDX microanalysis was performed on selected samples. On SEM micrographs the mean grain size of the matrix grains was measured through the method of Hilliard: $d = C/LM$ where C is the length of a circumference, L the number of grain boundaries on C and M the magnification.

For TEM observations, disc-shaped samples were mechanically ground up to 80 μm in thickness using 6 μm diamond paste in order to minimize the damage (micro-cracking) introduced in the sample during preparation. The samples were dimpled to 10 μm, then thinned by ion-milling (Ar^+, 6 kV). A Jeol 2010 equipped with a Link analyser EDS System and a HREM Topcon EM 002B (200 kV, $C_s = 0.4$ mm) were used. The chemical analyses were carried out using a probe size of 10 nm.

The following mechanical properties were measured:

- Vickers microhardness (HV1.0) measured on polished surfaces using a Zwick 3112 hardness tester, according to the European Standard ENV 843.
- Fracture toughness (K_{Ic}) evaluated with the same apparatus with a load of 98 N using the version of Anstis *et al.*'s formula as proposed by Zhao *et al.* [12].
- The Young modulus E measured through the resonance frequency method according to the European Standard ENV 843-2 on specimens $28.0 \times 8.0 \times 0.8$ mm^3 (length × width × thickness).
- Room Temperature flexural strength, in 4-point bend fixture on chamfered bars $2 \times 2.5 \times 25$ mm^3, with 20 and 10 mm as outer and inner span respectively, using a crosshead speed of 0.5 mm/min.

3. Results and discussion

3.1. Characteristics of the nanosized SiC powders

In Fig. 1a and b TEM micrographs of SiC powder are shown. SiC1 presents dispersed particles, while in SiC2 the particles are agglomerated forming long chains.The results of chemical analysis are reported in Table I. The resulting SiO_2 amount is about 6.8 wt% for SiC1 and 7.4 wt% for SiC2. Assuming the value of 2.45 g/cm^3 for the density of silica, the mean silica layer thickness on the SiC particles, estimated from the specific surface area, is 0.7 and 0.5 nm for SiC1 and SiC2 respectively. In Fig. 2a a HRTEM of a 20 nm particle of SiC2 is shown, revealing a 1 nm thick silica layer on the surface.

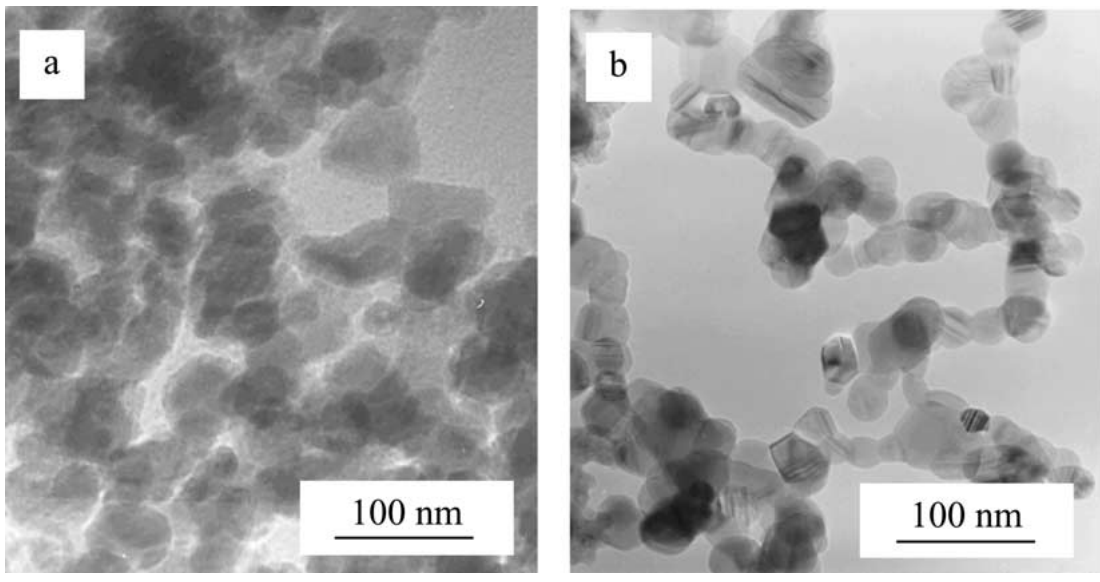

Figure 1 TEM images of the starting SiC powders. (a) SiC1, 45 nm, (b) SiC2, 30 nm.

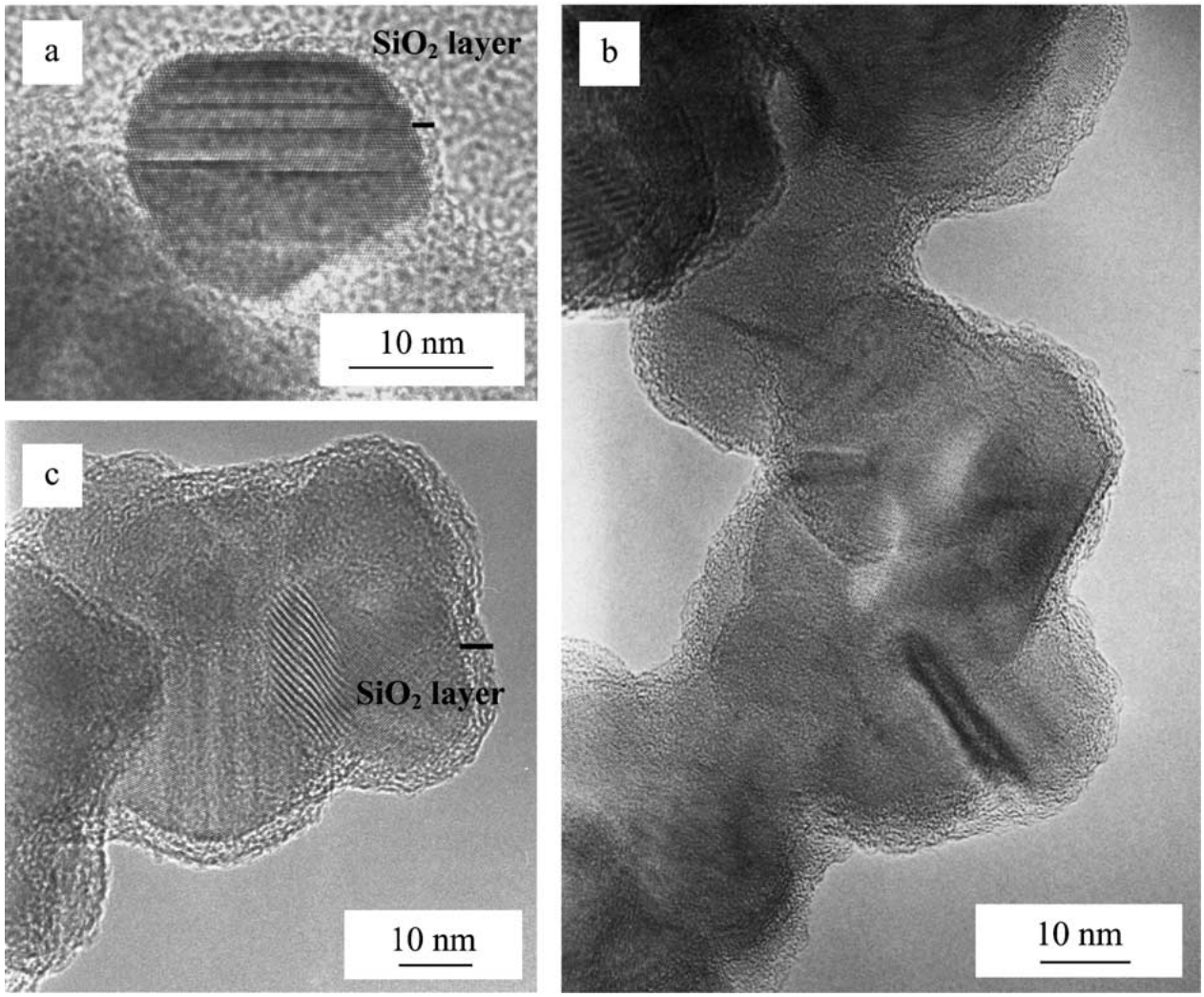

Figure 2 HRTEM micrographs of powder SiC2. (a) as received, (b) after thermal treatment at 1300°C/12 h/Ar, (c) after treatment in aqueous environment (R.T, pH = 6).

After the thermal cycle under argon, the oxygen content increased in both SiC powders, probably because a very low partial pressure of oxygen (2×10^{-1} Pa) was present in the furnace. At the same time a carbon loss occurred. The measured values are reported in Table I. In Fig. 2b, a HRTEM micrograph of SiC2 after thermal treatment reveals the silica layer.

The variation in the surface chemical composition of powder SiC2 after the treatment in water (R.T., 12 h, pH = 6) is revealed from the oxygen amount that is related to SiO_2 amount and the surface layer thickness (Table I). The results indicate that this treatment increased the amount of oxygen from 3.9 to 6.2 wt%. The surface layer thickness is shown in the HRTEM micrograph of Fig. 2c. This test proved that water-free solvents have to be used for the preparation of the powder mixture, in order to avoid oxygen enrichment.

3.2. Sintering behaviour of Al_2O_3-SiC powder mixtures

As previously mentioned, both pressureless sintering and hot pressing tests were carried out to evaluate the nanocomposite sinterability. The maximum final density achieved through pressureless sintering was 92% of relative density. The thermal cycle at $T = 1600$–1700°C in Ar, induced a substantial grain coarsening of Al_2O_3 particles, but sintering was very poor. An example of the low degree of densification reached by the nanocomposite containing 5% SiC after 1 hour at 1600°C under argon, is shown in Fig. 3. Some necks connecting alumina grains are visible, but substantial grain growth without sintering occurred. Increasing the temperature to 1800°C, no improvement of the final density was obtained and the densification was associated to a weight loss, due to the reaction of SiO_2 with SiC [9]:

$$SiC + 2SiO_2 \rightarrow 3SiO(g) + CO(g)$$

No densification was obtained when flowing N_2 was adopted for these tests. In contrast, monolithic alumina is normally densified to full density by pressureless sintering at 1550°C in air.

Although nanocomposites are generally very difficult to densify by pressureless sintering, some authors did succeed in producing dense materials, using SiC powders with grain size of about 150 nm, that is 4–5 times larger than the SiC used in this study [6]. In other words, for the same volumetric fraction of the second phase, the number of particles in the present case is about 2 orders of magnitude higher than in the materials found in literature. The SiC particles and their

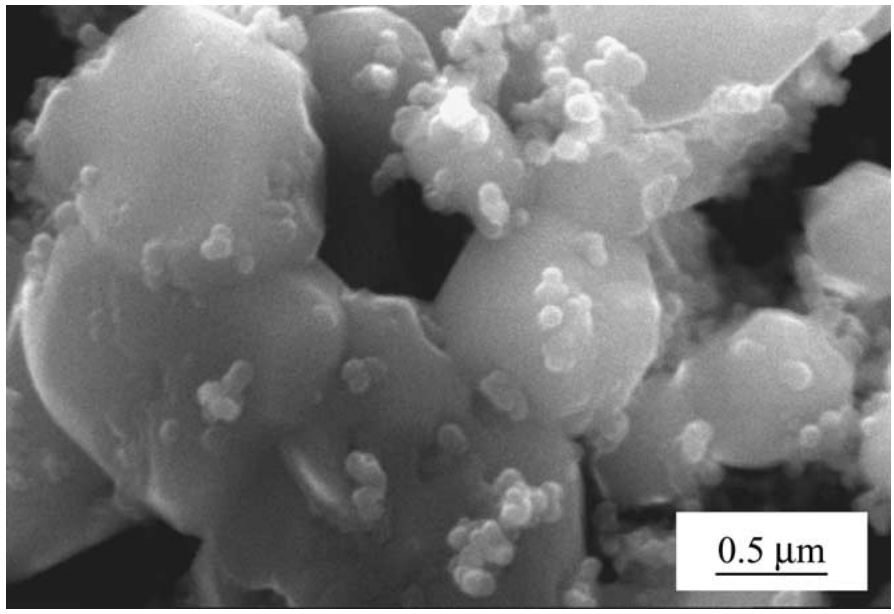

Figure 3 Low degree of densification in the nanocomposite containing 5% SiC after 1 hour at 1600°C under argon.

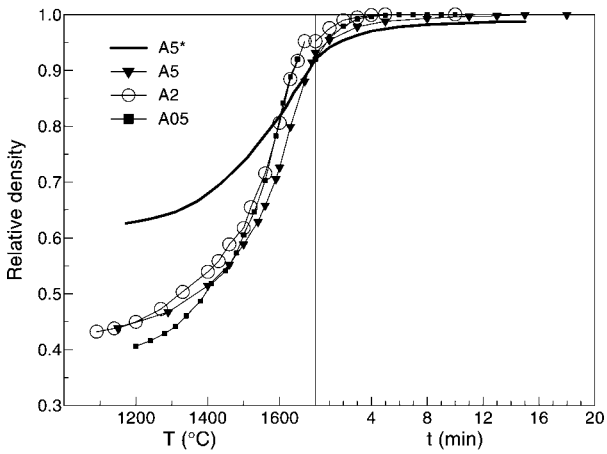

Figure 4 Densification behaviour of the nanocomposite powder mixtures.

agglomerates (visible around the alumina grains in Fig. 3) strongly retarded the densification mechanisms, by hindering the grain boundary movement.

Fully dense materials were obtained by hot pressing. The comparison of the densification behaviour, evaluated by the increase of density versus time/temperature (Fig. 4), confirms that the presence of silicon carbide particles lowers the sintering rate, therefore higher temperatures in respect to monolithic alumina are required to obtain fully dense materials, as already observed [1, 2, 6]. Similar densification behaviour was found for the nanocomposites produced with the same starting raw materials (A5, A2, and A0.5).

The influence of the type of Al_2O_3 powder is revealed comparing the densification behaviour of mixtures A5* and A5 (Fig. 4). As the powder mixtures were prepared in the same way, the difference is related to the characteristics of the raw materials: in the case of A5*, the higher mean particle size of the *coarse* Al_2O_3 (Table I) led to a better particle packing and consequently a higher green density (62% against 40–45%). On the other hand, the mixture A5 started to shrink at a lower temperature, due to the initial shrinkage step of particle rearrangement and, subsequently, showed a higher densification rate. At the beginning of the isothermal stage, all the mixtures reached more than 90% of relative density.

Although for these systems solid state sintering is considered as the main mechanism for densification, the presence of a high amount of silica in the starting SiC powder may have favoured the formation of a liquid phase and consequently a liquid-aided sintering process could have locally occurred. SEM and TEM observations confirmed the presence of amorphous liquid phase located at triple junctions, as explained in Section 3.

The SiC particles should be inert and non-sintering during the consolidation process. However, for higher SiC volume agglomerations, their partial sintering promoted by liquid silicate glass may have led to formation of larger particles.

3.3. Microstructure

3.3.1. SEM analysis

The fracture surfaces of the nanocomposites (see an example in Fig. 5) confirm an evident change of the fracture mode from completely intergranular (typical of alumina) to a mixture of inter- and trans-granular. The fraction of transgranular fracture increased with increasing amount of second phase. From the SEM images of polished surfaces it was ascertained that little or no residual porosity is present. The typical microstructure of the nanocomposites is shown in Fig. 6, presenting a SEM micrograph of sample A2 after polishing and thermal etching at 1350°C. SiC particles are predominantly located along the matrix grain boundaries, while only a small amount was found inside the grains. As the majority of particles in SiC2 appear linked together in the starting powder, they tend to form agglomerates also in the final products (particularly in A5 and A2). These clusters can be the origin of defects, like microcracks. In A5* sample, a better distribution

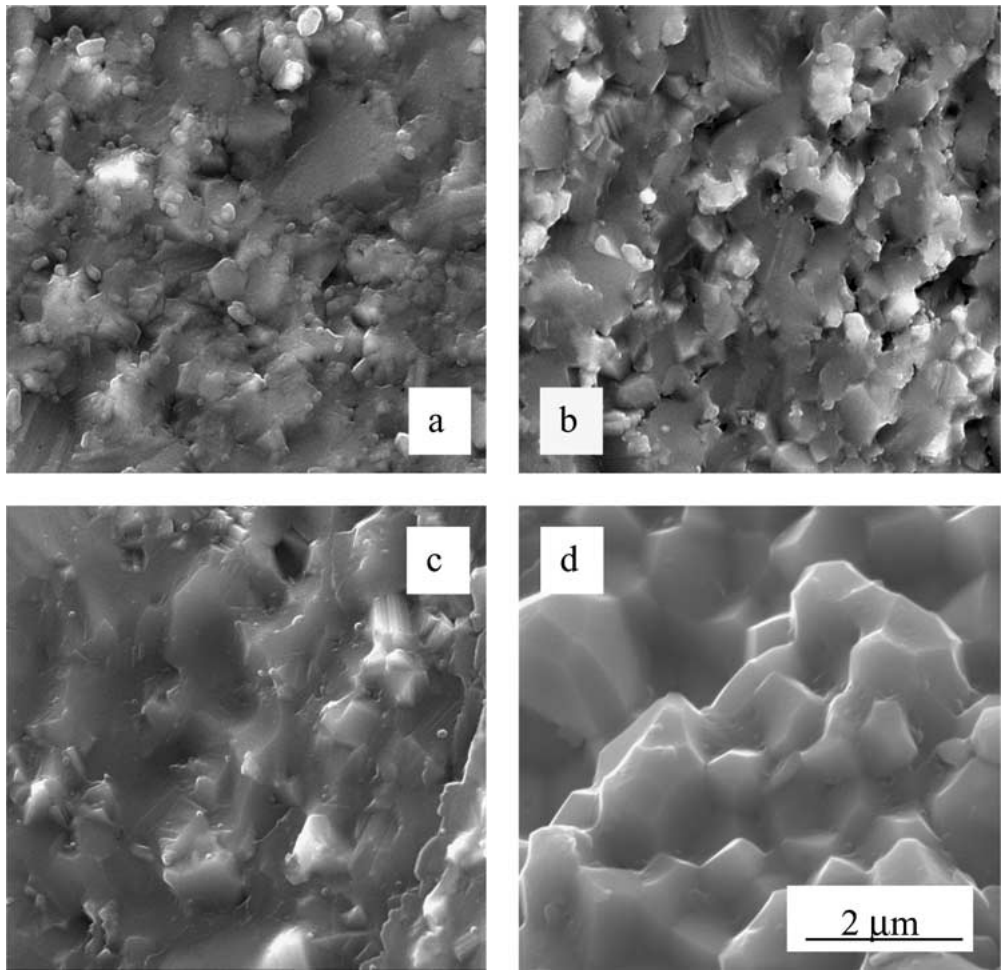

Figure 5 Fracture surfaces of (a), A5, (b) A2, (c) A0.5 and (d) alumina.

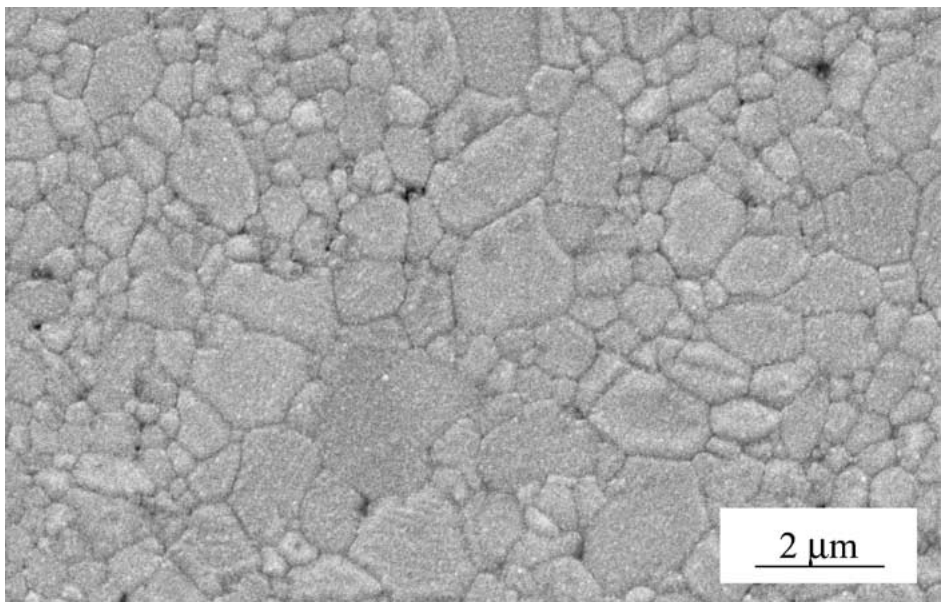

Figure 6 SEM micrograph of sample A2 after polishing and thermal etching at 1350°C.

of SiC particles along grain boundaries with little or no agglomerations was observed due to the dispersion and de-agglomeration of the particles in SiC1 powder. As a consequence, no microcracks formed during sintering and microstructural evolution.

The mean grain size values, reported in Table II, confirm the tendency to decrease with increasing SiC volume fraction, as reported by many authors [1, 2, 6, 13–15]. The grain size distribution is not homogeneous in the dense specimens containing SiC2: in A0.5 sample for instance, groups of grains with dimensions ranging from 1.5 to 1.7 μm are surrounded by regions of smaller grains with mean size from 0.3 to 0.5 μm. Similarly in A2, groups of 1 to 1.4 μm grains were observed as

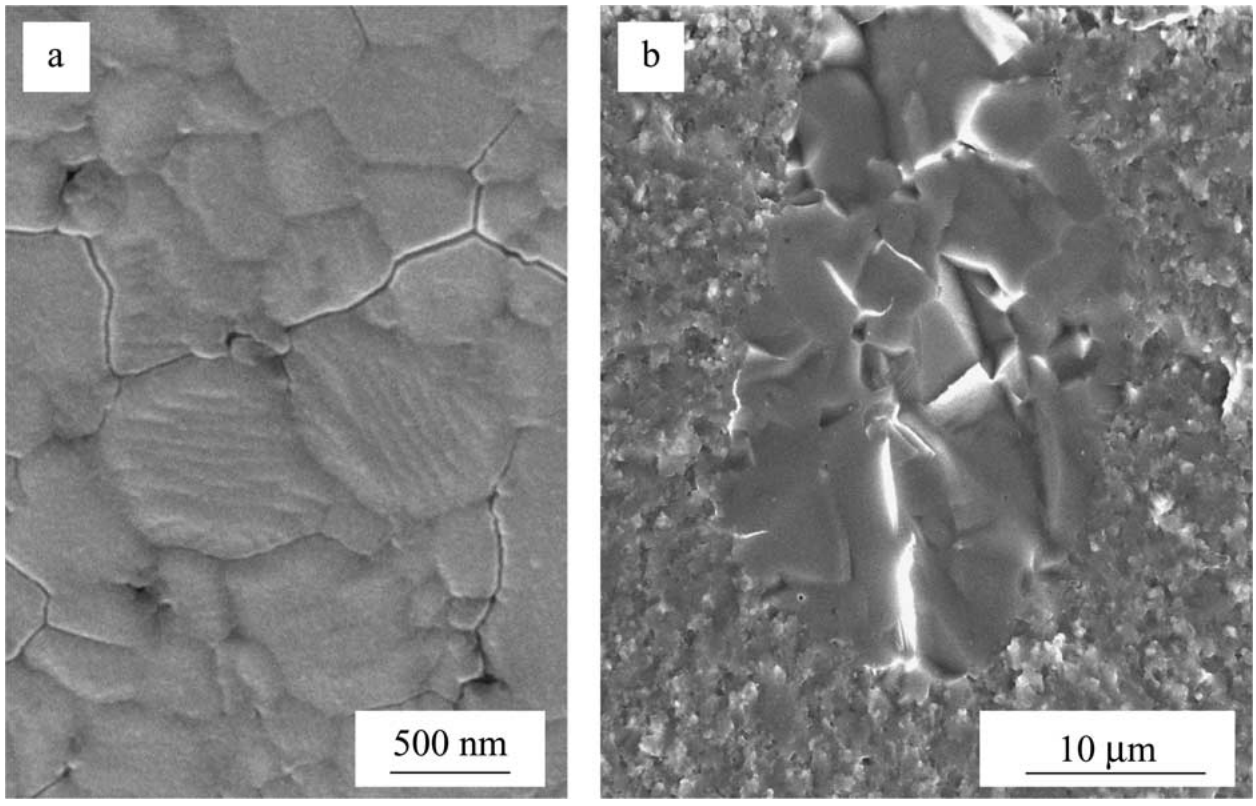

Figure 7 (a) Thermal etched surface of A5 showing microcracking along grain boundaries. (b) Abnormal alumina grain growth in the fracture surface of A5*.

well as 0.3–0.5 μm grains (see Fig. 6). Finally in A5 a certain inhomogeneity was observed too, due to a not perfect mixing of the starting powders.

On thermal etched surfaces microcracks were observed. The microcracks propagate along the grain boundaries and arise during cooling from thermal expansion coefficient mismatch between SiC and alumina. These cracks were not found in sample A5* and were attributed to the fact that SiC2 particles are agglomerated (Fig. 7a).

Comparing the systems A5 and A5*, that have the same SiC volumetric fraction but different starting alumina powders, the same matrix mean grain size was found, irrespective of the different Al_2O_3 powder grain size. Moreover the final dimensions of the matrix grains were not influenced by the size and the state of agglomeration of the SiC particles. Occasionally, in sample A5* abnormal alumina grain growth (up to 30 μm) was observed. An example is shown in Fig. 7b, representing a fracture surface resulting from flexural strength tests. These defects were probably due to the presence of large agglomerates in the starting coarse alumina powder, as they were not observed in the materials prepared with the fine Al_2O_3. The exaggerated grain growth could also have been favoured by the presence of a SiO_2-rich liquid phase.

3.3.2. TEM analysis

Additional microstructural features were revealed by TEM analyses, performed on nanocomposites produced from SiC2. The example shown in Fig. 8, relative to the sample A5, confirms that SiC particles are predominantly (>90%) located along the matrix grain boundaries, while only very small particles (about 20 nm) are entrapped inside the alumina grains. The agglomerates of SiC particles often surround a pore which can be open or act as a sink for the accumulation of excess amorphous phase. Otherwise, SiC grains are packed together along grain boundary forming polycrystals, having dimensions up to 500 nm. The SiC mean grain size is about 50 nm. Large pockets of SiC grains associated with porosity are frequently observed in triple junctions. Small agglomerates containing less than 10 particles can also be found inside the alumina grains. Observing the crystals under dynamic conditions (Bragg conditions), strain contrast is visible around intragranular SiC particles, as shown in Fig. 9. Thermal expansion coefficient mismatch between alumina and SiC causes local residual stresses that induce the strain observed. No microcracks were observed around intragranular SiC particles.

A triple junction observed is shown in Fig. 10. The SiC grains exhibit numerous stacking faults. They are well faceted and seem to be embedded inside a glassy phase. On the other hand, a certain amount of glassy phase is expected to have formed due to the high content of SiO_2 in the starting SiC powders (Table I). EDS microanalysis was performed inside the pocket containing SiC nanocrystals, shown in Fig. 10 (size of analysed areas $\sim$15 nm). The composition of the intergranular phase (containing mainly Al, Si, and O) seems to be heterogeneous, but it is difficult to determine the exact composition as the contribution of the surrounding Al_2O_3 grains cannot be excluded.

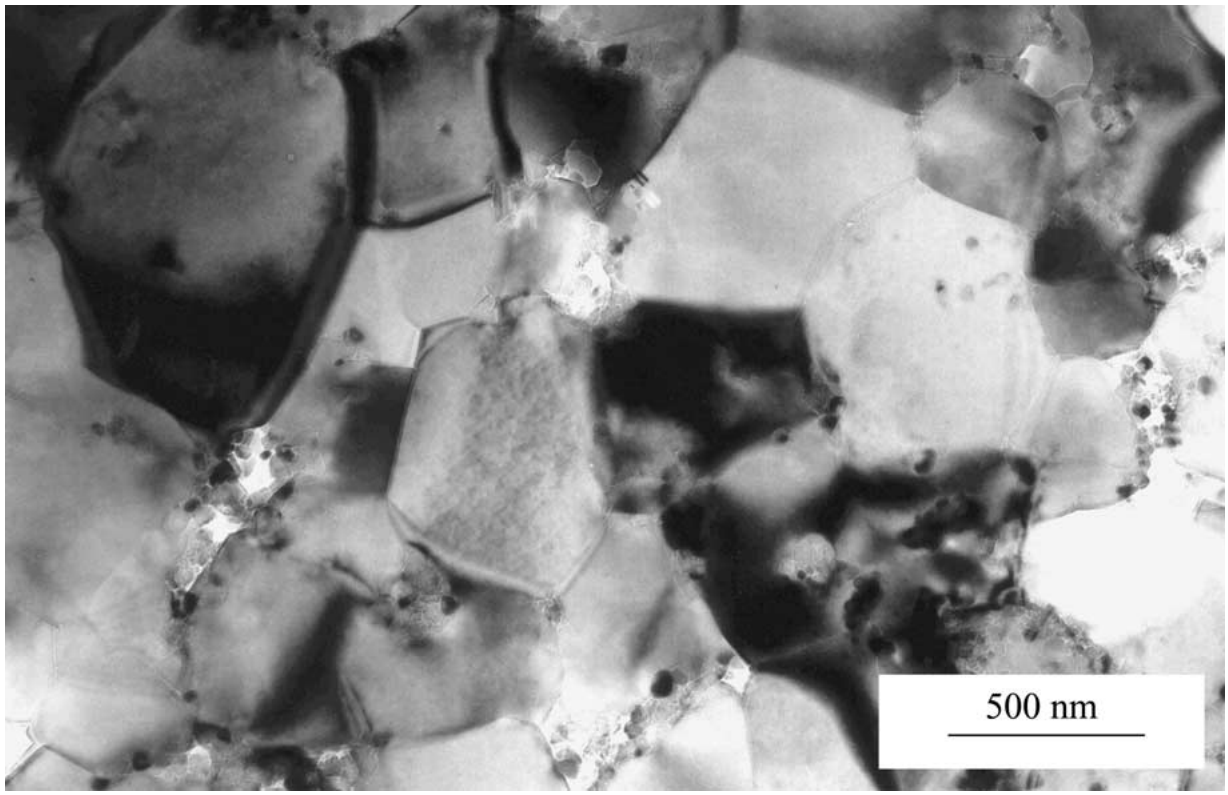

Figure 8 Distribution of SiC particles in A5. SiC particles are predominantly located along the matrix grain boundaries.

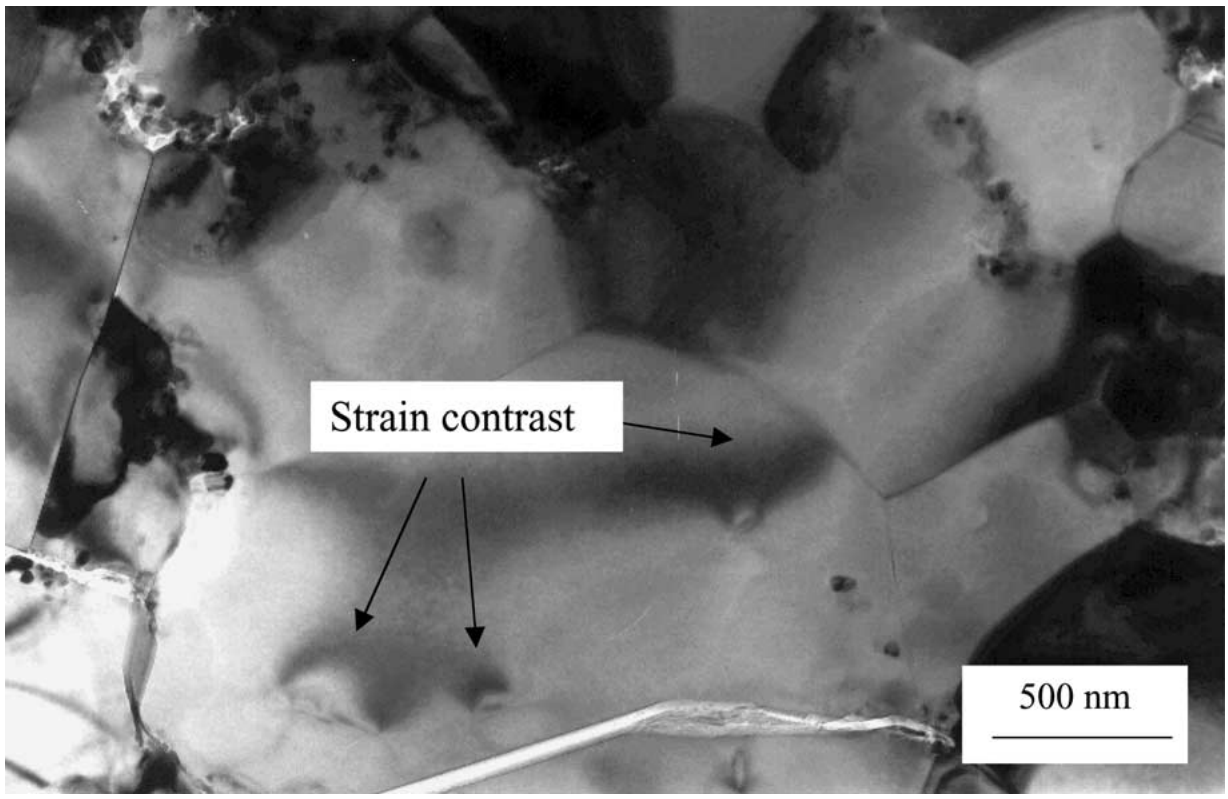

Figure 9 Sample A5. Strain contrast around intragranular SiC due to thermal expansion coefficient mismatch between alumina and SiC.

In Fig. 11 a HRTEM micrograph of the SiC/Al_2O_3 interface is shown. In this case the phase boundary is free from amorphous phase. However, the presence of thin films (2 nm thick) at these boundaries cannot be excluded [9] even if the liquid phase accumulates preferentially in large pockets and pores in the open space between large SiC particle agglomerates. The micrograph in Fig. 11 suggests strong adhesion between the particle and the matrix in the A5 nanocomposite. This is in agreement with the change in fracture path from intergranular in pure alumina to transgranular in the composites.

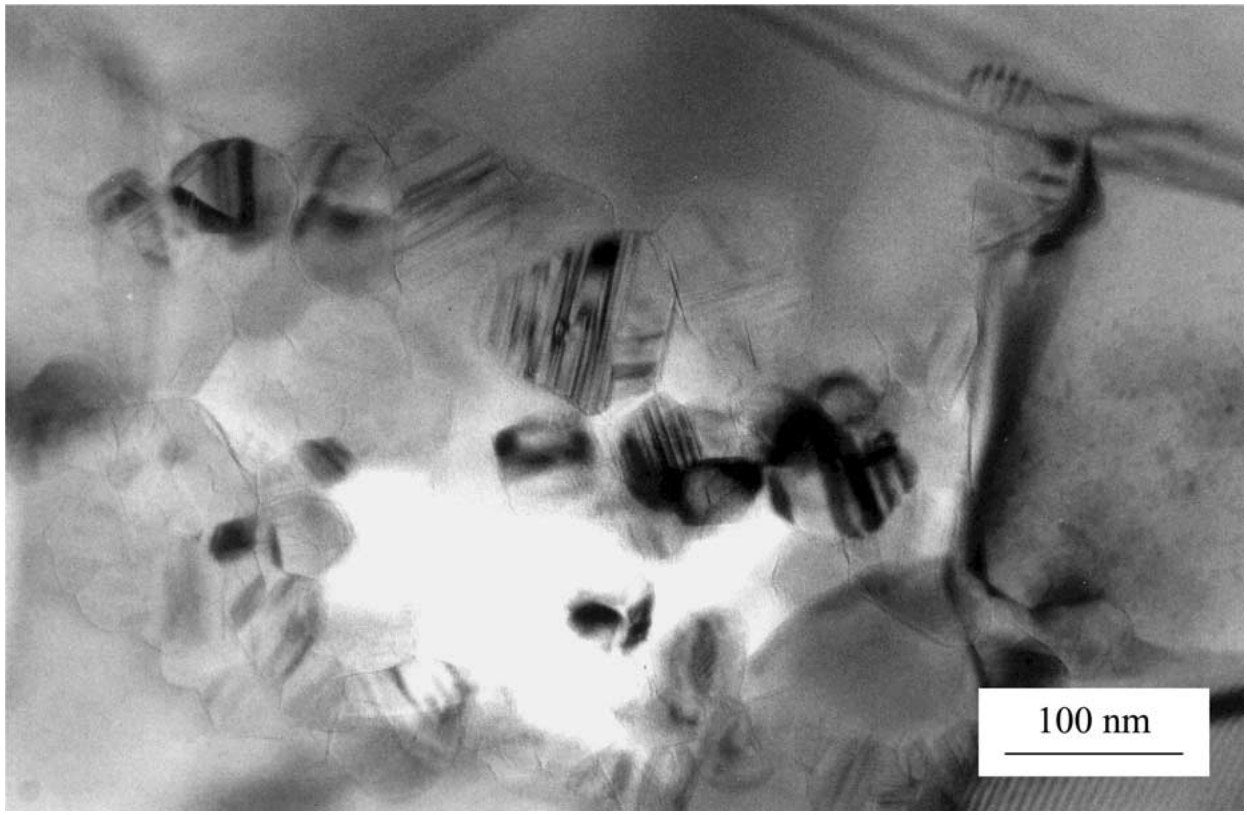

Figure 10 Sample A5. High magnification micrograph of a triple junction. The SiC grains exhibit numerous stacking faults and are embedded inside a glassy phase.

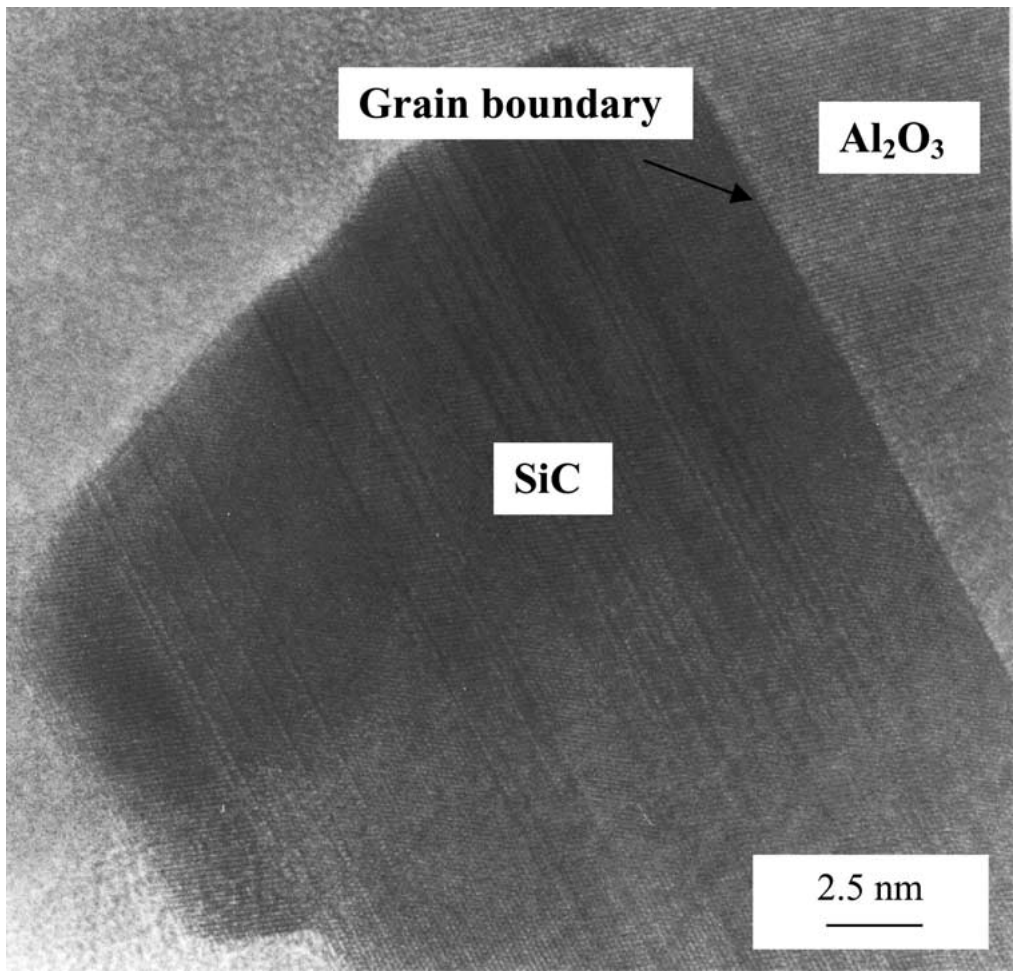

Figure 11 Sample A5. HRTEM picture of a SiC/Al_2O_3 interface. The phase boundary is free from amorphous phase.

4. Mechanical properties

The results are summarized in Table III. For comparison, the properties of the monolithic alumina are also reported. All nanocomposites show a slightly increased hardness over monolithic alumina. Comparing the systems with the same SiC volumetric fraction, namely A5 and A5*, the values can be considered statistically the same. Theoretically, assuming a linear rule of mixtures, by adding 5% SiC an increase of about 0.5 GPa is expected. Moreover according to this rule, hardness is expected to increase with increasing the SiC volumetric fraction. This trend was approximately confirmed by the experimental values obtained.

The Young modulus values are lower than one would expect on the basis of the rule of mixtures. In the case of sample A5*, considering the values of 396 GPa for alumina and 420–440 GPa for SiC, an increase of about 2 GPa should be observed for nanocomposites. Similarly, for the materials produced with SiC2, the Young modulus is observed to decrease with increasing particulate fraction. Possible explanations, related to microstructural features, are: (a) the presence of grain boundary silicate phases, which possess a low value of elastic modulus and (b) the presence of intergranular microcracking due to residual stresses between the matrix grains and SiC agglomerates.

The fracture toughness of A5* sample was observed to increase of about 40% over monolithic alumina. This can be explained simply by the change in fracture mode from intergranular to transgranular, which implies a reinforcement of the grain boundary. It has been estimated that the toughness increase solely due to the change of fracture mode is about 1.58 K_o, where K_o is the fracture toughness of monolithic alumina [23].

In the case of materials produced starting from SiC2 (A5, A2 and A0.5), the toughness values are lower than those of the corresponding alumina independently on the added volumetric fraction and despite the change in fracture mode. The crack path was straight and its length longer than in alumina. The fracture mode change was not effective in the present case. The presence of microcracks, which is often considered as a toughening mechanism, was detrimental for these materials, probably as a consequence of the number and dimensions of these defects. Conflicting results and theories are reported in literature about the grain boundary strengthening and toughening [1, 12, 21, 22, 25]. According to Niihara [1–3] and concerning toughening effects, SiC particles should be located inside the alumina grains. However, as illustrated in the previous sections, in the materials of the present study, SiC particles are located preferentially along the grain boundaries.

Moreover, the materials presented by Niihara should be considered submicron-sized and not nano-sized composites, as the SiC particle dimensions range from 100 to several hundred nm and the matrix grain size in the composite containing 5 vol% SiC is about 1–2 μm [2, 3]. Therefore the theories about mechanisms governing grain growth and densification and subsequently microstructure and mechanical properties may not be suitable for finer materials, as the ones presented in this study. The toughness data, measured on ceramic composites having both the matrix and the second phase of nano-size dimensions, do not sustain any of the toughening mechanism previously suggested [21, 22]. More likely, in agreement with the assumptions of Pezzotti *et al.* [22, 24] our results validate the hypothesis that toughnening effects are not achievable by the nanocomposite approach: dispersoids much larger than the nanometer scale would be needed to obtain tangible benefits in terms of intrinsic toughness. In fact positive effects were obtained when using particulate having dimensions from 0.5 μm to some micrometers [1, 13, 23]. Finally, as the specimens were polished up to 1 μm before being indented, the measured toughness values are not affected by residual stresses due to machining, in contrast with the results reported by Zhao *et al*. [12].

Flexural strength increased from 430 to 642 (49%) for the A5* system produced with the SiC1. SEM analyses of the fracture surfaces revealed that the critical defects were agglomerates of Al_2O_3 grains (see Fig. 7b). An estimation of the flaw size C of both A5* and A was performed through the Griffith equation $\sigma = Y\, K_{IC}/C^{1/2}$, where Y is the geometrical factor that depends on flaw shape [26]. Different shape factors were considered and the values obtained are reported in Table III. Through a simple comparison of the experimental values, one concludes that the increment of strength over monolithic alumina can be attributed to both the increase of toughness and decrease of the critical flaw in the nanocomposite, which, in turn, is related to matrix grain size refinement.

In the case of nanocomposites produced with SiC2, no beneficial effect was observed concerning strength. In contrast with the results reported in the literature, the strength values were observed to decrease with increasing the fraction of added particles. A possible

TABLE III Mechanical properties

		Mechanical properties						
						Flaw size* (μm)		
Sample	m.g.s. (μm)	HV1.0 (GPa)	E (GPa)	K_{IC} (MPa*m$^{1/2}$)	σ (MPa)	I	II	III
A5*	0.34	20.4 ± 0.4	357 ± 4	3.8 ± 0.2	642 ± 102	21	19	15
A*	1.2	18.7 ± 0.6	396	3.0 ± 0.2	430 ± 37	28	25	19
A5	0.3–0.4	20.1 ± 0.4	368 ± 4	2.9 ± 0.1	403 ± 29	32	28	22
A2	0.4–0.5	20.9 ± 0.5	367 ± 4	2.7 ± 0.1	477 ± 21	20	17	13
A0.5	~0.6	19.1 ± 0.4	379 ± 4	2.9 ± 0.2	423 ± 75	29	25	20
A	~0.9	18.3 ± 0.5	380 ± 4	3.5 ± 0.2	575 ± 142	23	20	15

*Calculated from Griffith equation, at different flaw shape: I Semicircle $c = a$, II Semiellipse $c = 1.4a$, III semiellipse $c = 2a$.

explanation for this kind of behaviour is again, the presence of microcracks that in many regions nearly form a network, and the presence of SiC particle aggregates and consequent porosity. This hypothesis is based on the following observations:

- The lowest value of strength was found for the system A5 that exhibited the highest number of cracks.
- This sample showed a large number of SiC agglomerates at triple points (on TEM images).
- In most of the fracture surfaces of these materials, it was not possible to identify the critical flaw giving rise to the sample rupture.
- Cracks form along the grain boundary, as confirmed by microstructural analysis, in agreement with previous studies on composites with intergranular particles [27].

The critical flaw size, obtained through the Griffith equation, increases over monolithic alumina. If the sample rupture was caused by microcracks, this means that cracks were almost connected and extended over regions as large as several tens of μm. The decrease of strength in these materials is therefore due to both the low toughness and the increase of flaw size dimensions.

The results obtained show a considerable difference in mechanical behaviour between systems A5 and A5*, containing the same volume fraction of SiC particles. This does not depend on the matrix mean grain size and grain size distribution that are quite similar. In addition both systems exhibit a change in the fracture mode from intergranular to transgranular. The main factor determining the difference in mechanical performance is therefore related to the different features of SiC starting powders and their dispersion in the dense materials. In sample A5, the presence of SiC agglomerates prevented complete densification and affected all mechanical properties, particularly strength and fracture toughness. In theory, a decrease of grain size should lead to an increase in strength. However, the composites containing SiC2 were subjected to an additional source of internal stresses, the thermal expansion coefficient mismatch between matrix and particles agglomerates. Therefore in the case of A5 (as well as A2, A0.5), the positive effects of the fine microstructure were overcome by the presence of an extended microcracking.

In contrast, no or little amount of SiC agglomeration was found in sample A5*, prepared from SiC1, therefore strength benefits from grain size refinement.

Finally, it is not possible to attribute the improvement of strength observed for A5* to an apparent toughening of the material due to compressive stresses introduced by machining operations, as all the bars for strength tests were cut and machined following the same procedure.

The observed strength behaviour is related to the relationship between processing flaws and particle size. In fact, all the nanocomposites present flaws typical in size of micron and sub-micron ceramics: large alumina particles, microcracks, and crack-like voids due to SiC agglomerates. Size and volume density of these flaws depend on the processing routes and are inversely dependent on the particle size of the raw powders.

5. Conclusions

An extensive study on Alumina-Silicon Carbide nanocomposites was carried out, concerning analysis of raw materials, processing, microstructural and mechanical characteristics. A range of different compositions was produced and studied and different kinds of raw materials were used. Chemical analyses and TEM observations were performed on SiC powders to determine the amount of oxygen and its enrichment after treatment in water. As a result, water-free solvents were preferred for powder processing.

The sintering tests confirmed that these systems have a poor sinterability due to the presence of SiC particles that hinder the densification mechanisms. Nearly full dense materials were obtained by hot pressing, while very low densities resulted after pressureless sintering.

SEM and TEM observation of the microstructure confirmed that SiC particles affect the matrix grain size, as already found in the literature. The mechanical tests showed in some cases improvement of mechanical performance but also degradation with respect to monolithic alumina.

This study has pointed out that not only the composition but, to a large extent, the type of nanopowders and the processing procedure are the fundamental factors affecting the characteristic of the final products. The predominant effect of SiC is related to the high number of particles per unit volume, that interfere with densification and grain growth mechanisms, creating obstacles to the grain boundary movement during sintering and defects where they agglomerate, like porosity and stress accumulation. Processing flaws acting as critical defects under mechanical stresses overcome potential positive effects due to the very fine microstructures like those designed in Al_2O_3-SiC in ceramic nanocomposites.

Acknowledgements

This work was carried out in the frame of the EU project BETCT97-0592–Thematic Network Nanomat. The Authors thank Dr. E. Borsella (ENEA-Frascati, Italy) and Dr. N. Herlain (CEA-Saclay, France), for the preparation of the nanosized SiC powders.

References

1. K. NIIHARA, *J. Ceram. Soc. Japan (Int. Ed.)* **99** (1991) 945.
2. A. NAKAHIRA and K. NIIHARA, *J. Ceram. Soc. Jpn.* **100** (1992) 448.
3. T. HIRANO, A. NAKAHIRA and K. NIHARA, *J. Amer. Ceram. Soc.* **79** (1996) 33.
4. K. NIHARA and A. NAKAHIRA, in Ceramics: Towards the 21st century. The Ceram. Soc. of Japan (1991) p. 404.
5. M. STERNITZKE, *J. Europ. Ceram. Soc.* **17** (1997) 1061.
6. L. C. STEARNS, J. ZHAO and M. P. HARMER, *ibid.* **10** (1992) 473.
7. C. E. BORSA, S. JIAO, R. I. TODD and R. J. BROOK, *J. Microscopy* **177** (1995) 305.
8. C. E. BORSA, N. M. R. JONES, R. J. BROOK and R. I. TODD, *J. Europ. Ceram. Soc.* **17** (1997) 865.
9. H. K.SCHMID, M. ASLAN, S. ASSMANN, R. NASS and H. SCHMIDT, *ibid.* **18** (1998) 39.

10. D. ZHANF, H. YANG, R. YU and W. WENG, *J. Mater. Sci. Lett.* **16** (1997) 877.
11. L. CARROLL, M. STERNITZKE and B. DERBY, *Acta Mater.* **44** (1996) 4543.
12. J. ZHAO, L. C. STEARNS, M. P. HARMER, H. M. CHAN and G. A. MILLER, *J. Amer. Ceram. Soc.* **76** (1993) 503.
13. Z.-Y.-DENG, J.-L. SHI, Y.-F. ZHANG, D.-Y. JIANG and J.-K. GUO, *J. Europ. Ceram. Soc.* **18** (1998) 501.
14. L. C. STEARNS and M. P. HARMER, *J. Amer. Ceram. Soc.* **79** (1996) 3013.
15. Y. XU, A. ZANGVIL and A. KERBER, *J. Europ. Ceram. Soc.* **17** (1997) 921.
16. A. J. WINN and R. I. TODD, *British Ceramic Proceedings* **59** (1999) 153.
17. H. WOHLFROMM, *Ceramic Processing Science and Technology, Ceramic Transaction* **51** (1995) 659.
18. C. E. BORSA and R. J. BROOK, *ibid*. **51** (1995) 653.
19. A. PICIACCHIO, S. HO LEE and GARY L. MESSING, *J. Amer. Ceram. Soc.* **77** (1994) 2157.
20. D. SCITI, D. DALLE FABBRICHE and A. BELLOSI, in "Key Engineering Materials," edited by J. Baxter, L. Cot, R. Fordham, V. Gabis, Y. Hellot, M. Lefebvre, H. Le Doussal, A. Le Sech, R. Naslain and A. Sevagen (Trans Tech Publication, June 1997) Vols. 132–136, p. 2001.
21. G. PEZZOTTI, T. NISHIDA and M. SAKAI, *J. Ceram. Soc. Jpn.* **103** (1995) 901.
22. G. PEZZOTTI, V. SERGO, K. OTA, O. SBAIZERO, N. MURAKI, T. NISHIDA and M. SAKAI, *J. Ceram. Soc. Jpn.* **104** (1996) 497.
23. D. O'SULLIVAN, M. POORTEMAN, B. THIERRY, A. LERICHE, P. DESCAMPS and F. CAMBIER, *Silicates Industriel* **11/12** (1996) 235.
24. I. LEVIN, W. D. KAPLAN and D. G. BRAINDON, *J. Amer. Ceram. Soc*. **78** (1995) 254.
25. J. FANG, M. P. HARMER and H. M. CHAN, *J. Mater. Sci.* **32** (1997) 3247.
26. Y. MURAKAMI, in "Stress Intensity Factors Handbook" (Pergamon Press, Oxford, 1987) Vol. 1, p. 42.
27. A. ZIMMERMANN, M. HOFFMAN and J. RÖDEL, *J. Mater. Res.* **15** (2000) 107.

Received 3 April 2001
and accepted 24 January 2002